Mechanism of Lipid Nanodrop Spreading in a Case of Asymmetric Wetting

Sawsan Mohamad, Olivier Noël, Jean-Luc Buraud, Guillaume Brotons, Yasmina Fedala, and Dominique Ausserré*

UMR CNRS 6283, "Molecular Landscapes, Biophotonic Horizons" Group, Université du Maine, Le Mans, France

(Received 31 August 2012; published 14 December 2012)

Using the surface enhanced ellipsometric contrast microscopy, we follow the last stage of the spreading of egg phosphatidylcholine nanodroplets on a hydrophilic substrate in a humid atmosphere, focusing on the vanishing trilayer in terraced droplets reduced to coexisting monolayer and trilayer. We find that the line interface between them exhibits two coexisting states, one mobile and one fixed. From there, it is possible to elucidate the internal structure and the spreading mechanism of the stratified liquid in a case of asymmetric wetting, i.e., where the lipid film is made of an odd number of leaflets.

DOI: 10.1103/PhysRevLett.109.248108 PACS numbers: 87.14.Cc, 61.30.Hn, 61.30.Jf, 47.45.Dt

In proper temperature and vapor pressure conditions, pure amphiphilic molecules most often self-assemble in symmetric lamellar stacks with bilayered repeat unit. In practice, the spreading of amphiphilic molecules such as lipids [1], symmetric block copolymers [2], or liquid crystals [3–6] on solid surfaces in air is a major aspect in controlling the shape and behavior of very small volumes of materials on surfaces, which has presently important issues, such as surface vesicle fusion, surface patterning, elaboration of biomimetic membranes, microcontact printing [7,8], or biochip spotting [9]. In the case of phospholipids, most of the studies are conducted at the solid-liquid interface [10–12], because of the great potential of these molecules to make scaffolds for biochips [13–15]. It requires that the polar part of the molecules is exposed towards the water, which cannot be obtained by spreading them on any surface in air. Lipid films on a hydrophilic substrate in water correspond to the so-called symmetric wetting situation [16,17], where the number of monolayer leaflets in the supported film is even, due to the preferential affinity of both the solid and the liquid with the polar head of the molecules. In this case, spreading has been described as the rolling of the front bilayer creeping on the solid surface [18–21]. The same mechanism does not transpose to the asymmetric wetting situation [16,22–24], where the solid and the free surface prefer to be in contact with opposite parts of the molecule (hydrophilic versus hydrophobic). Then, the creeping front layer is a monolayer, which cannot roll on itself. Therefore, by contrast with the symmetric case, its spreading cannot be envisaged without considering its topological interaction with the stratified reservoir. To our knowledge, the spreading mechanism has not been described in this case. The aim of the present Letter is to fill this gap. Asymmetric wetting is encountered with lipid droplets on a hydrophilic substrate in air or on a hydrophobic substrate in water. The number of leaflets is odd, and the thinnest possible films are one and then, three lipid leaflets thick. In this context, the work reported herein this Letter presents three specificities: it deals with phospholipid films spreading on hydrophilic surfaces in air, hence with asymmetric wetting; the experiments are conducted in a humid atmosphere so that the samples are partially hydrated, which favors homogeneity and lateral fluidity [25]; it addresses very small lipid droplets (typically 1 μm^3). Such drops quickly evolve towards trilayered patches surrounded by a monolayer. Using the surface enhanced ellipsometric contrast [26–28] with an optical microscope working at a fixed magnification, the history of every molecular layer can be properly traced from this stage to the final structure, which is a single molecular monolayer disk with typically 200 μm diameter. Over most of the experiment duration, coexistence of a monolayer and a trilayer is observed. The difference between the two regions is one bilayer (about 5 nm thick). It is bordered by a dislocation line along its edge, that is to say along the trilayer-monolayer interface. In this Letter, we show that two states are coexisting along this line, which we will qualify liquid and solid. From there, we are able to describe the internal structure of the spreading film and to elucidate the spreading mechanism for the asymmetric lipid stack.

In our experiments, nanodrops of the egg phosphatidylcholine (Egg PC) lipid mixture (Avanti Polar Lipids, Inc.) were deposited on a hydrophilic oxidized silicon surface with 106 nm SiO_2 in order to use the surface enhanced ellipsometric contrast microscopy. Through this layer, the polarization state of the light is only weakly affected upon reflection, which allows us to obtain a good extinction of the substrate between cross polarizers, hence to visualize added molecular layers in reflection with an excellent contrast [26]. Drop deposition was made in ambient atmosphere and then drop spreading was observed in a humid atmosphere, with a 70% relative humidity set by equilibrating the sample with a saturated NaCl solution in a glove bag. Five series of images illustrating the trilayer evolution are displayed in Fig. 1. They correspond to independent experiments, with increasing drop size. The second series is spread over two lines in order to illustrate once the end of the wetting process. In each image, the intensity of a region is approximately a linear function of

 © 2012 American Physical Society

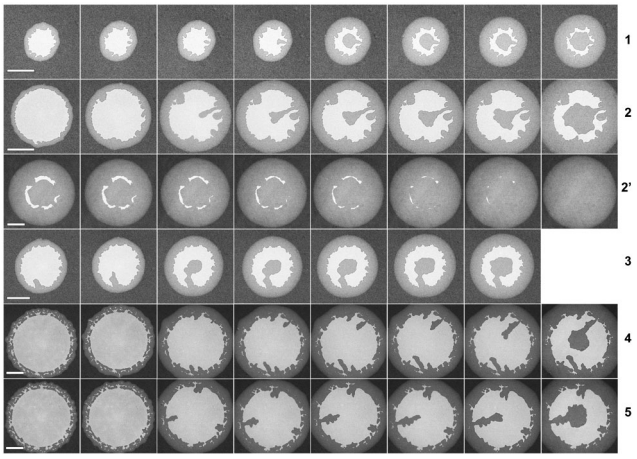

FIG. 1. Five spreading trilayer kinetics. Scale bar is 50 μm everywhere. The duration of each series is, respectively, 3h38, 4h11, 2h30, 2h03, 5h52, and 4h05. Series 2′ is the continuation of 2, after a time lapse of 2h38. Image contrast has been nonlinearly enhanced.

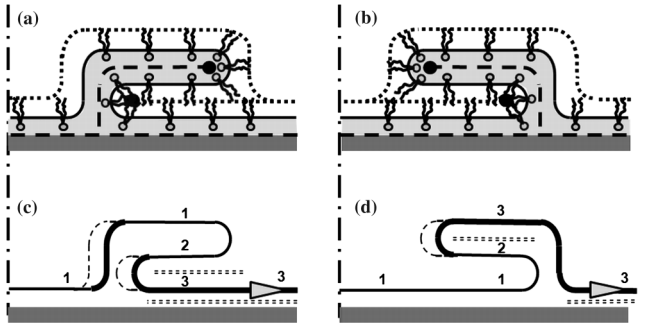

FIG. 2. (a),(b) The two possible internal structures of a nanodrop with coexisting monolayer and trilayer. The vertical dash-dotted line represents the central axis of the drop; gray areas are hydrophilic domains; dotted lines represent either tail-tail or tail-air interfaces; dashed lines represent head-head interfaces. The snaking solid line holds for the head-tail interface. U-turns of the solid lines are the edges of the trilayer. Dislocation lines, normal to the section, are marked by a large dot in the dislocation heart. (c),(d) The corresponding interfacial flow during the spreading is suggested by the gray arrow. Thin solid line: fixed parts of the interface; dashed line and thick solid line: previous and new position of the moving parts; thin double line: slipping planes.

the optical film thickness [27]. Brightest regions are trilayers, gray regions such as the droplet corona are single monolayers and dark surrounding regions are the bare substrate. The trilayer shrinks, leaving a monolayer at its place, so what actually shrinks is a bilayer. At the beginning of this process, invaginations form at the edge of the trilayer and progress towards the center. When one invagination reaches the center, its extremity enlarges and becomes a circular monolayer domain surrounded by the trilayer, the internal edge thus formed, and the external edge of the trilayer being roughly concentric. The central monolayer domain grows up at the expense of the trilayer until the latter totally disappears. During this process, the spreading monolayer progresses outwards while keeping a perfectly circular shape. This is quite surprising because it is fed by the receding trilayer, which has no radial symmetry due to the existence of a canal connecting the internal and external monolayers. Even more intriguing is that most of the outwards trilayer edge line remains frozen while shrinking.

We assume that a vertical section of the spreading drop during trilayer receding conforms to one of the two schemes given in Figs. 2(a) and 2(b). The structure is a twice-folded monolayer. The left and right U-turns of the solid line correspond to dislocations positioned at a different height in the trilayer stack, that we name the upper and the lower dislocations. Their composition is different. Their core is, respectively, filled with polar heads and water molecules, or with the aliphatic chains. Were the two dislocation lines at the same height, the monolayer and the additional bilayer would be disconnected and the only mechanism by which they could exchange material would be permeation, which is expected to be hindered in a humid atmosphere [29–31]. In our experiments, molecular exchange between adjacent monolayers is supposed to occur exclusively via the dislocation lines, which directly connect each pair of adjacent leaflets [29]. Figures 2(c) and 2(d) differ from Figs. 2(a) and 2(b) by a time interval Δt. They illustrate how the trilayer unfolds when the external monolayer spreads. According to our experimental observations, we impose a fixed trilayer external edge. Indices 1, 2, and 3 are attributed to the various leaflets in the trilayer stack in view of their topological relationship with the central monolayer. Molecules of the internal monolayer cannot move and leaflet 1 has a zero velocity with respect to the solid surface. Leaflet 3 has the highest velocity among all the leaflets. The way the trilayer unfolds is just determined by the balance between relative layer-layer and layer-solid friction coefficients in the stack. The friction of the outwards monolayer against the solid regulates the overall spreading rate but does not interfere with the unfolding mechanism. The absence of motion of the outwards dislocation tells us that the slipping plane is 2–3 in both Figs. 2(c) and 2(d). It was shown in several studies [19,32,33] that friction between leaflets with facing aliphatic parts of the molecules was ten to hundred times larger than friction between leaflets with facing polar heads or between polar heads and the hydrated solid. Therefore, the highest friction is between leaflets 2 and 3 in Fig. 2(c) and between leaflets 1 and 2 in Fig. 2(d). As a consequence, the only scheme which is consistent with our experiments is that of Fig. 2(d) (and Fig. 2(b)).

Figure 3 presents the superimposition of two pictures of the same drop extracted from the second series in Fig. 1 and snapped at different times. It reveals two distinct behaviors along the trilayer edge line, fixed or moving. The fixed regions are principally located along the outwards edge. They do not even smooth out with time and

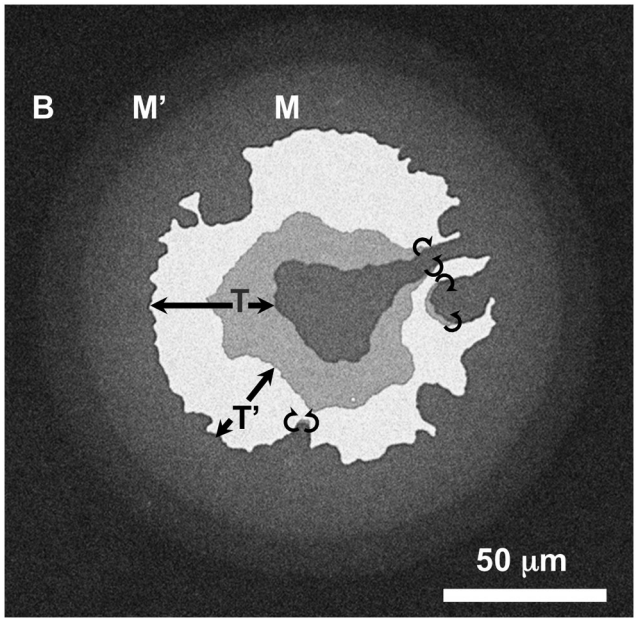

FIG. 3. Superimposition of two semitransparent images of the same drop, (series 2 and 2′ in Fig. 1) taken with a time interval t'-t of 1h52. From dark to bright, we find B the bare substrate, $M'$and M the monolayer at t' and t (starting from the center), $T'$and T the trilayer at t' and t (extension shown by double arrow). The black half-circle-arrows mark the point defects separating mobile and fixed contour arcs along the trilayer edge.

behave as a one-dimensional solid. The moving parts of the trilayer edge are those feeding the outwards spreading monolayer. According to the mechanism illustrated in Fig. 2(d), they correspond to upper dislocations. From there, monolayer 3 flows over the lower dislocation at the external bilayer edge into the external monolayer. Hence, moving contour arcs in Fig. 3 correspond to upper folds with polar cores and fixed arcs correspond to lower folds with aliphatic cores. Since the two states alternate along the continuous bilayer edge, they must be connected by some point defect. We imagine a screw dislocation. Hence, it comes with a given chirality, so there should be two types of such point defects that we may qualify clockwise and anticlockwise. Since the external edge is principally frozen in position and shape, we can infer that invaginations are triggered by the formation of a pair of dual (clockwise and anticlockwise) point defects, which allow formation and growth of a moving arc between them. The precise description of these point defects remains an interesting open problem. Another puzzling question is why a lower type dislocation line does not move at all. Indeed, independently of the spreading process, we would have expected that it would have at least smoothed out with time due to line tension, but this was not observed. The explanation that we propose refers to similar spreading trilayers in 8CB smectic liquid crystals on hydrophilic surfaces, which also lead to asymmetric wetting situations. It was shown [34] that in ambient conditions the external spreading monolayer is in a gaseous state, hence diffusing everywhere over the solid surface, while the same monolayer in the trilayer stack is in a liquid state. Similarly, we can imagine that a lipid leaflet is liquid when it is exposed to the air but that it becomes solid when it is confined between the solid and upper monolayers. Phase transition displacements in the first layers against the solid were previously reported in supported lipid stacks [35–37]. They were attributed to the surface potential exerted by the solid. Similar displacements between free and covered monolayers on a same substrate can be expected from interactions with the upper layers. Then, the solid or liquid character of the lower and upper dislocation lines would just, respectively, reflect the solid state of the leaflet against the solid and the liquid state of the one or the two upper leaflets. This hypothesis strengthens the topological description of Fig. 2(b) compared to Fig. 2(a). Moreover, it explains why the external edge of the additional bilayer is strictly immobile. Indeed, on the sole basis of the balance between competing 1–2 and 2–3 friction coefficients, we would have expected some, even if tiny, displacement of the external edge, which was not observed.

Figure 4 shows what happens when the deposited drop is larger than those shown in Fig. 1. Instabilities develop outwards during trilayer spreading and form wormlike filaments (Fig. 4, left) which detach from the central trilayer during the late stage to ultimately dissolve into the surrounding monolayer (Fig. 4, right). These filaments vanish without any change in their shape, as can be checked by comparing Fig. 4, left and Fig. 4, right. It suggests that their edge is solidlike, enclosing a lower dislocation, and that this is the equilibrium state. By contrast, during the same time interval, the monolayer surrounding the filaments significantly

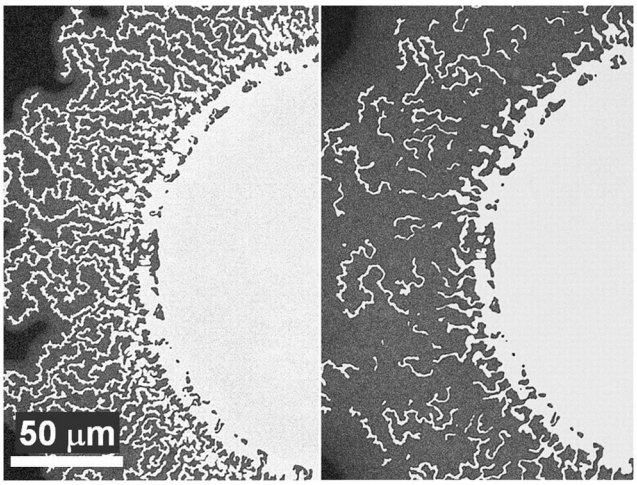

FIG. 4. Larger spreading drops than those of Fig. 1 exhibit wormlike trilayer filaments due to spreading instabilities. Left and right snapshots are separated by a time interval of 1h44. The bright regions are trilayers, the gray region surrounding the filaments is a single monolayer, and the darker region is the bare solid surface.

extends over the surface, demonstrating very different molecular mobility. Compared to monolayer spreading, filament vanishing is, therefore, a very slow process, which occurs necessarily through weak molecular permeation.

On the whole, considering that the trilayer is the sum of a monolayer and a bilayer, we understand that the equilibrium location of the dislocation line at the edge of this bilayer is below the monolayer, and that it reversibly switches to the upper level when required by the spreading flow. Thus, the bilayer edge is solid at equilibrium and adopts a stationary liquid state under the flow. It is worth pointing out that, although the trilayer edge is continuous and closed, the bilayer component is ill-defined, since it is locally composed of either the two upper or the two lower leaflets, depending if the edge is locally liquid or solid. Phase coexistence along the continuous edge of a bilayer step might be a general phenomenon in amphiphilic films, and describing the structure and evolution of ultrathin smectic systems in terms of switchable defect lines, is hopefully an interesting approach. More generally, we claim that flows and defects are indivisible in strongly stratified materials, since they condition each other. In diblock copolymers for instance, this approach might help to decrypt the formation and disappearance of islands and holes in annealed ultrathin films [38] and to understand the evolution of the characteristic cone shaped droplets which spontaneously form in these systems [39–41]. The spreading mechanism described in the present Letter as a snakelike interface unfolding in a specific case of lipid asymmetric wetting might also apply to the other one (hydrophobic surface in water). It also raises new questions on symmetric wetting situations. Indeed, the rolling mechanism proposed previously by Rädler *et al.* [18] is only part of the spreading problem, the other part being the connection of the spreading bilayer with the layered reservoir.

This work was supported by ANR Program No. PNANO07-050.

*dominique.ausserre@univ-lemans.fr

[1] J. Jass, T. Tjarnhage, and G. Puu, Biophys. J. **79**, 3153 (2000).
[2] V. A. Belyi and T. A. Witten, J. Chem. Phys. **120**, 5476 (2004).
[3] O. Benichou, M. Cachile, A. M. Cazabat, C. Poulard, M. P. Valignat, F. Vandenbrouck, and D. Van Effenterre, Adv. Colloid Interface Sci. **100-102**, 381 (2003).
[4] Y. L. Zhao, N. Erina, T. Yasuda, T. Kato, and J. F. Stoddart, J. Mater. Chem. **19**, 3469 (2009).
[5] A. J. McDonald and S. Hanna, Phys. Rev. E **75**, 041703 (2007).
[6] L. Xu, M. Salmeron, and S. Bardon, Phys. Rev. Lett. **84**, 1519 (2000).
[7] A. N. Parikh, Biointerphases **3**, 1 (2008).
[8] O. A. Nafday, T. W. Lowry, and S. Lenhert, Small **8**, 1021 (2012).
[9] Y. Deng *et al.*, J. Am. Chem. Soc. **130**, 6267 (2008).
[10] G. E. G. Jothi, S. Kamatchi, and A. Dhathathreyan, J. Chem. Sci. **122**, 341 (2010).
[11] M. L. Hisette, P. Haddad, T. Gisler, C. M. Marques, and A. P. Schröder, Soft Matter **4**, 828 (2008).
[12] L. Limozin and K. Sengupta, Biophys. J. **93**, 3300 (2007).
[13] E. Sackmann, Science **271**, 43 (1996).
[14] E. T. Castellana and P. S. Cremer, Surf. Sci. Rep. **61**, 429 (2006).
[15] M. Bally, K. Bailey, K. Sugihara, D. Grieshaber, J. Vörös, and B. Städler, Small **6**, 2481 (2010).
[16] N. Singh, A. Kudrle, M. Sikka, and F. S. Bates, J. Phys. II (France) **5**, 377 (1995).
[17] E. Huang, S. Pruzinsky, T. P. Russell, J. Mays, and C. J. Hawker, Macromolecules **32**, 5299 (1999).
[18] J. Rädler, H. Strey, and E. Sackmann, Langmuir **11**, 4539 (1995).
[19] B. Sanii, K. Nguyen, J. O. Rädler, and A. N. Parikh, ChemPhysChem **10**, 2787 (2009).
[20] P. Jonsson, J. P. Beech, J. O. Tegenfeldt, and F. Hook *et al.*, J. Am. Chem. Soc. **131**, 5294 (2009).
[21] I. Gozen, P. Dommersnes, I. Czolkos, A. Jesorka, T. Lobovkina, and O. Orwar, Nat. Mater. **9**, 908 (2010).
[22] M. A. Holden, S.-Y. Jung, T. Yang, E. T. Castellana, and P. S. Cremer, J. Am. Chem. Soc. **126**, 6512 (2004).
[23] M. C. Howland, A. R. Sapuri-Butti, S. S. Dixit, A. M. Dattelbaum, A. P. Shreve, and A. N. Parikh, J. Am. Chem. Soc. **127**, 6752 (2005).
[24] J. M. Solletti, M. Botreau, F. Sommer, W. L. Brunat, S. Kasas, T. M. Duc, and M. R. Celio, Langmuir **12**, 5379 (1996).
[25] T. Baumgart and A. Offenhauser, Biophys. J. **83**, 1489 (2002).
[26] D. Ausserre and M. P. Valignat, Nano Lett. **6**, 1384 (2006).
[27] D. Ausserre and R. Abou Khachfe, Langmuir **23**, 8015 (2007).
[28] O. Noel, J.-L. Buraud, L. Berger, and D. Ausserre, Langmuir **26**, 6015 (2010).
[29] W. K. Chan and W. W. Webb, Phys. Rev. Lett. **46**, 603 (1981).
[30] W. K. Chan and W. W. Webb, J. Phys. (Paris) **42**, 1007 (1981).
[31] A. A. Gurtovenko and I. Vattulainen, *Handbook of Modern Biophysics* (Humana, Totowa, NJ, 2009).
[32] W. H. Briscoe, S. Titmuss, F. Tiberg, R. K. Thomas, D. J. McGillivray, and J. Klein, Nature (London) **444**, 191 (2006).
[33] B. Sanii and A. N. Parikh, Soft Matter **3**, 974 (2007).
[34] S. Bardon, R. Ober, M. Valignat, F. Vandenbrouck, A. Cazabat, and J. Daillant, Phys. Rev. E **59**, 6808 (1999).
[35] Z. V. Feng, T. A. Spurlin, and A. A. Gewirth, Biophys. J. **88**, 2154 (2005).
[36] A. Charrier and F. Thibaudau, Biophys. J. **89**, 1094 (2005).
[37] D. Keller, N. B. Larsen, I. M. Moller, and O. G. Mouritsen, Phys. Rev. Lett. **94**, 025701 (2005).
[38] M. W. Matsen, Curr. Opin. Colloid Interface Sci. **3**, 40 (1998).
[39] A. B. Croll, M. V. Massa, M. W. Matsen, and K. Dalnoki-Veress, Phys. Rev. Lett. **97**, 204502 (2006).
[40] J. U. Kim and M. W. Matsen, Soft Matter **5**, 2889 (2009).
[41] T. H. Kim, J. Huh, and C. Park, Macromolecules **43**, 5352 (2010).